Photon subtracted squeezed states generated with periodically poled $KTiOPO_4$

Kentaro Wakui, Hiroki Takahashi

National Institute of Information and Communications Technology (NICT), 4-2-1 Nukui-Kita, Koganei, Tokyo 184-8795, Japan and Department of Applied Physics, School of Engineering, The University of Tokyo, 7-3-1 Hongo, Bunkyo-ku, Tokyo 113-8656, Japan

kwakui@nict.go.jp

Akira Furusawa

Department of Applied Physics, School of Engineering, The University of Tokyo, 7-3-1 Hongo, Bunkyo-ku, Tokyo 113-8656, Japan

Masahide Sasaki

National Institute of Information and Communications Technology (NICT), 4-2-1 Nukui-Kita, Koganei, Tokyo 184-8795, Japan

Abstract: We present generation of photon-subtracted squeezed states at 860 nm, from nearly pure, continuous-wave squeezed vacua generated with a periodically-poled $KTiOPO_4$ crystal as a nonlinear medium of a subthreshold optical parametric oscillator. We observe various kinds of photon-subtracted squeezed states, including non-Gaussian states similar to the *single-photon state* and *superposition states of coherent states*, simply by changing the pump power. Nonclassicality of the generated states clearly shows up as its negative region around the origin of the phase-space distributions, i.e., the Wigner functions. We obtain the value, -0.083 at the origin of the Wigner function, which is largest ever observed without any correction for experimental imperfections.

OCIS codes: (270.0270) Quantum optics; (270.6570) Squeezed states.

References and links

1. H.-A. Bachor and T. C. Ralph, *A Guide to Experiments in Quantum Optics* (WILEY-VCH Verlag GmbH & Co. KGaA, 2004).
2. C. C. Gerry and P. L. Knight, *Introductory Quantum Optics* (Cambridge University Press, 2005).
3. S. L. Braunstein and A. K. Pati, *Quantum Information with Continuous Variables* (Kluwer Academic Publishers, 2003).
4. B. Yurke and D. Stoler, "Measurement of amplitude probability distributions for photon-number-operator eigenstates," Phys. Rev. A **36**, 1955-1958 (1987).
5. M. Dakna, T. Anhut, T. Opatrný, L. Knöll, and D.-G. Welsch, "Generating Schrödinger-cat-like states by means of conditional measurements on a beam splitter," Phys. Rev. A **55**, 3184-3194 (1997).
6. U. Leonhardt, *Measuring the quantum state of light* (Cambridge University Press, 1997).
7. A. I. Lvovsky, H. Hansen, T. Aichele, O. Benson, J. Mlynek, and S. Schiller, "Quantum State Reconstruction of the Single-Photon Fock State," Phys. Rev. Lett. **87**, 050402/1-4 (2001).
8. A. Zavatta, S. Viciani, and M. Bellini, "Tomographic reconstruction of the single-photon Fock state by high-frequency homodyne detection," Phys. Rev. A **70**, 053821/1-6 (2004).
9. A. Ourjoumtsev, R. Tualle-Brouri, Ph. Grangier, "Quantum homodyne tomography of a two-photon Fock state," Phys. Rev. Lett. **96**, 213601/1-4 (2006).

#78885 - $15.00 USD Received 10 January 2007; revised 1 March 2007; accepted 2 March 2007

10. A. I. Lvovsky, and S. A. Babichev, "Synthesis and tomographic characterization of the displaced Fock state of light," Phys. Rev. A **66**, 011801(R)/1-4 (2002).
11. A. Zavatta, S. Viciani, and M. Bellini, "Quantum-to-Classical Transition with Single-Photon-Added Coherent States of Light," Science **306**, 660-662 (2004).
12. A. Ourjoumtsev, R. Tualle-Brouri, J. Laurat, and Ph. Grangier, "Generating Optical Schrodinger Kittens for Quantum Information Processing," Science **312**, 83-86 (2006).
13. J. S. Neergaard-Nielsen, B. Melholt Nielsen, C. Hettich, K. Mølmer, and E. S. Polzik, "Generation of a Superposition of Odd Photon Number States for Quantum Information Networks," Phys. Rev. Lett. **97**, 083604/1-4 (2006).
14. H. Mabuchi, E. S. Polzik, and H. J. Kimble, "Blue-light-induced infrared absorption in KNbO3," J. Opt. Soc. Am. B **11**, 2023 (1994).
15. T. Aoki, G. Takahashi, and A. Furusawa, "Squeezing at 946 nm with periodically poled $KTiOPO_4$," Opt. Express **14**, 6930-6935 (2006).
16. S. Suzuki, H. Yonezawa, F. Kannari, M. Sasaki, and A. Furusawa, "7 dB quadrature squeezing at 860 nm with periodically poled $KTiOPO_4$," Appl. Phys. Lett. **89**, 061116/1-3 (2006).
17. E. S. Polzik, J. Carri, and H. J. Kimble, "Atomic spectroscopy with squeezed light for sensitivity beyond the vacuum-state limit," Appl. Phys. B: Photophys. Laser Chem. **55**, 279-290 (1992).
18. R. W. P. Drever, J. L. Hall, F. V. Kowalski, J. Hough, G. M. Ford, A. J. Munley, and H. Ward, "Laser Phase and Frequency Stabilization Using an Optical Resonator," Appl. Phys. B **31**, 97-105 (1983).
19. A. I. Lvovsky, "Iterative maximum-likelihood reconstruction in quantum homodyne tomography," J. Opt. B: Quantum Semiclass. Opt. **6**, S556-S559 (2004).
20. M. Sasaki and S. Suzuki, "Multimode theory of measurement-induced non-Gaussian operation on wideband squeezed light: Analytical formula," Phys. Rev. A **73**, 043807/1-18 (2006).
21. K. Mølmer, "Non-Gaussian states from continuous-wave Gaussian light sources," Phys. Rev. A **73**, 063804/1-7 (2006).
22. S. L. Braunstein and H. J. Kimble, "Teleportation of Continuous Quantum Variables," Phys. Rev. Lett. **80**, 869-872 (1998).
23. N. Takei, N. Lee, D. Moriyama, J. S. Neergaard-Nielsen, and A. Furusawa, "Time-gated Einstein-Podolsky-Rosen correlation," Phys. Rev. A **74**, 060101(R)/1-4 (2006).
24. T. C. Ralph, A. Gilchrist, G. J. Milburn, W. J. Munro and S. Glancy, "Quantum computation with optical coherent states," Phys. Rev. A **68**, 042319/1-11 (2003).
25. E. Waks, E. Diamanti, B. C. Sanders, S. D. Bartlett, and Y. Yamamoto, "Direct Observation of Nonclassical Photon Statistics in Parametric Down-Conversion," Phys. Rev. Lett. **92**, 113602/1-4 (2004).
26. D. Rosenberg, A. E. Lita, A. J. Miller, and S. W. Nam, "Noise-free high-efficiency photon-number-resolving detectors," Phys. Rev. A **71**, 061803(R)/1-4 (2005).
27. M. Fujiwara and M. Sasaki, "Photon-number-resolving detection at a telecommunications wavelength with a charge-integration photon detector," Opt. Lett. **31**, 691-693 (2006).
28. A. P. Lund, H. Jeong, T. C. Ralph and M. S. Kim, "Conditional production of superpositions of coherent states with inefficient photon detection," Phys. Rev. A **70**, 020101(R)/1-4 (2004).
29. Note that the squeezing levels shown in this paper are for the quadrature observables defined by $\hat{X} = \int_{-\infty}^{\infty} dt \Psi_0(t)\hat{X}(t)$. They can be directly evaluated with the initial squeezed vacua right after the OPO, using a following expression; $2\langle \hat{X}^2 \rangle \equiv 1 - 2\frac{\gamma_T}{\zeta_0} \cdot \frac{z(z+3)}{(z+1)(z+2)^2}$. Here, $z = \sqrt{P/P_{th}}$ is normalized pump power where P is pump power and P_{th} is an oscillation threshold of the OPO.

1. Introduction

Generation of nonclassical states of light has been an important task for quantum optics experiments and optical quantum information processing. To date, a second-order nonlinear process has widely used because one can effectively generate such nonclassical states as squeezed states or entangled photon pairs via parametric down-conversion (PDC) [1, 2]. Compared to the second-order nonlinearity, third or higher order nonlinearity, e.g., Kerr nonlinearity, is very weak and not so frequently employed at a single-photon level. Such nonlinearities are, however, essential to exploit true potential of optical quantum information processing with continuous quantum variables such as the quadrature amplitudes of electromagnetic fields [3].

On the other hand, conditional state-preparation scheme has attracted attention recently. In conditional state-preparation schemes, strong nonlinearities can be induced by quantum measurements even at a single-photon level. However conditional they are, they can generate

#78885 - $15.00 USD Received 10 January 2007; revised 1 March 2007; accepted 2 March 2007

various nonclassical states via photon counting on subsystem of an entangled state produced in PDC [4, 5]. Generated states in such ways would be the Fock (photon number) states or similar states to superposition of coherent states - the optical analogs of Schrödinger-cat states. Nonclassicality of such states is specifically characterized by its negative region of the phase-space distribution functions, i.e., the Wigner functions. This is in sharp contrast to that of a squeezed state, which has a non-negative definite Gaussian distribution of the Wigner function. Here, the Wigner function $W(x,p)$, is defined as a quasi-probability distribution for non-commuting quadrature observables $\hat{x}\hat{p}-\hat{p}\hat{x}=i$ (with $\hbar=1$), and can directly be reconstructed by optical homodyne tomography [6].

Various nonclassical, non-Gaussian optical quantum states with negative values of $W(x,p)$ have been generated. Those states can be categorized into two families. One family is the Fock states and their variants combined with coherent states [7, 8, 9, 10, 11], created in a non-collinear PDC configuration of the signal and idler photons. The other is the photon-subtracted squeezed states, where a small fraction of a squeezed vacuum beam is beam-split and guided into a photon counter as trigger photons, and the remaining beam is conditioned by the detection of the trigger photons [5]. In the ideal case, a squeezed vacuum is a superposition of even photon-number states where the signal and idler photons are collinear, thus, one-photon-subtracted squeezed states must be a particular superposition of odd photon-number states. These states are close to optical Schrödinger-cat states with small coherent amplitudes, and thereby referred to as optical *"Schrödinger kittens"* [12, 13].

In the previous works of Schrödinger kittens, potassium niobate ($KNbO_3$) crystals are used as nonlinear optical media for an optical parametric amplifier (OPA) [12], or in an optical parametric oscillator (OPO) far below threshold [13]. In the case of experiments with $KNbO_3$, however, it is known that there is a big source of loss referred to as pump (blue) light induced infrared absorption (BLIIRA) [14]. The big loss caused by BLIIRA weakens the even-photon nature of a squeezed vacuum, that is to say, it weakens entanglement between two modes into which the squeezed vacuum is beam-split, and yields uncorrelated trigger photons. They induce false clicks in state preparation and consequently degrades the output conditioned states. The most negative value observed with $KNbO_3$ so far, is -0.026 without any corrections of experimental imperfections [12].

On the other hand, periodically-poled $KTiOPO_4$ (PPKTP) has been turned out not to have the BLIIRA effect in continuous-wave squeezing experiments [15, 16]. Therefore, a squeezing level at 860 nm has been significantly improved [16]. Thanks to its almost BLIIRA-free property, one can obtain squeezing with higher purity (even-photon nature) than that in the case of using $KNbO_3$. Purity of squeezing depends on how big portion of a squeezed vacuum can escape from an OPO cavity. The cavity escape efficiency, which can be calculated by a transmittance of an OPO output coupler and all intracavity losses [17], is $\sim$97 % with PPKTP while that of $KNbO_3$ is $\sim$80 % at most.

Here we also present that PPKTP is very useful to generate a wide range of the photon-subtracted squeezed states, including the single-photon state and Schrödinger kittens, with the deepest negative dips of the Wigner functions ever observed. The single-photon state can be realized to subtract one photon from a squeezed vacuum with a weakly pumped OPO [21], but could not be created in the previous photon-subtraction experiments due to the impure squeezed vacua generated with $KNbO_3$. The usage of PPKTP enables one to generate the states from the single-photon to Schrödinger kittens, by simply tuning the squeezing level which is directly controlled by the pump power for the squeezer.

#78885 - $15.00 USD Received 10 January 2007; revised 1 March 2007; accepted 2 March 2007

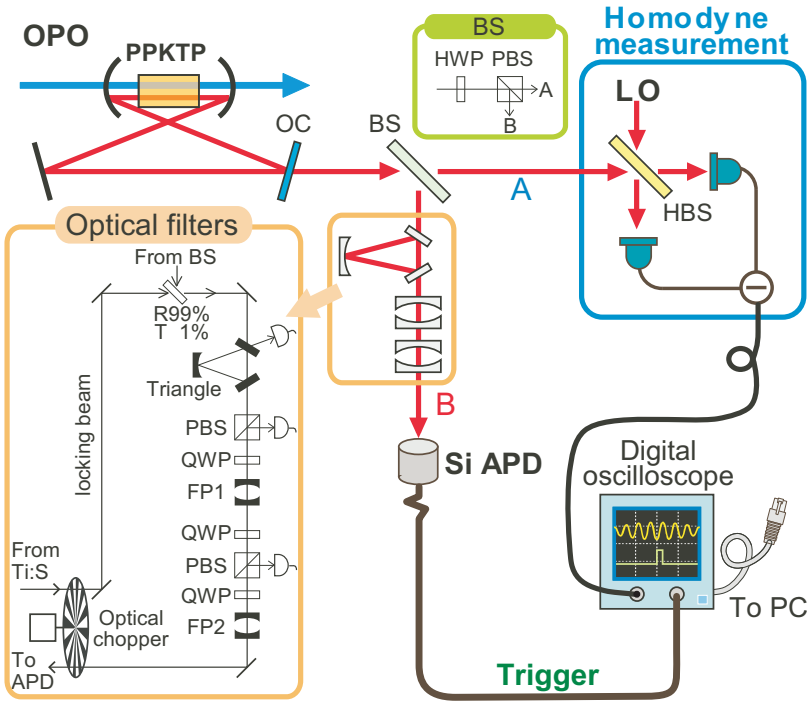

Fig. 1. Schematic of experimental setup. OC : output coupler, HWP : half-wave plate, PBS : polarizing beam splitter, BS : beam splitter (consisting of HWP and PBS, variable splitting ratio), Triangle : triangle cavity, QWP : quarter-wave plate, FP1 & FP2 : Fabry-Perot cavities, HBS : 50:50 beam-splitter. All the beams including the squeezed vacuum have S-polarization. The sets of PBS+QWP just before FP1 & FP2 are used as optical isolators and also as pick-offs of the reflected beams. Each reflection from the filtering cavities is used for FM-sideband locking when the locking beam passes through at the optical chopper.

2. Experimental setup

A schematic of our experimental setup is shown in Fig. 1. A continuous-wave Ti:Sapphire laser (Coherent MBR-110) is used as a primary source of the fundamental beam at 860 nm, which is mainly used to generate second harmonic (430 nm) of about 200 mW by a frequency doubler (a bow-tie cavity with $KNbO_3$). It is also used as a local oscillator (LO) for homodyne detection, and as probe beams for various control purposes. The second harmonic beam is used to pump the OPO with a 10 mm long PPKTP crystal (Raicol Crystals) as a nonlinear medium in an optical cavity (a bow-tie configuration with a round-trip length of about 523 mm). The output coupler (OC) of this squeezer cavity has a transmittance of 10.3 %. The intracavity loss is about 0.2∼0.3 %, which is nearly independent from the pump power and much better than that with $KNbO_3$ in our case (2 ∼ 3 %). The FWHM of the cavity is about 9.3 MHz. Note that above basic components for the generation of a squeezed vacuum are essentially the same as that in the setup showed in [16].

A small fraction (5 %) of the squeezed vacuum beam in path A is split at a beam splitter (BS), guided into a commercial Si-APD (Perkin Elmer SPCM-AQR-16) through three optical filtering cavities in path B, and is used as trigger signals for conditional photon subtraction. The finesses of the filtering cavities are about 60 (Triangle), 600 (FP1), and 1500 (FP2), respec-

#78885 - $15.00 USD Received 10 January 2007; revised 1 March 2007; accepted 2 March 2007

tively. All the filtering cavities have 5∼10 times wider bandwidths than that of the OPO. The spectrum of the trigger photons through these filters consists of a single peak around 860 nm at the degenerate mode with a bandwidth of 8.6 MHz (FWHM). Other irrelevant, nondegenerate, modes from the OPO, peaking at every free spectral range of 573 MHz apart from the degenerate frequency, are sufficiently well suppressed. The total transfer efficiency after the BS for the mode of interest is about 30 % just in front of the Si-APD. The trigger counting rate varies from less than 1 kcps up to 50 kcps, changing with the pump power of OPO from 1 mW up to 160 mW and splitting ratios. These trigger counting rates are mostly much greater than the Si-APD dark counts (100 cps).

Reducing background light is crucial for using an Si-APD because bright background light easily degrades signal-to-noise ratio of trigger photons. Usually weak coherent beams are used as references to lock optical cavities [16], but they directly yield vast amounts of counts. Therefore, one has to contrive ways to count photons and lock optical cavities in the same experimental setup.

We apply time sharing control of the system by a "sample-and-hold locking" technique, which enables us to switch the system from a "locking time-bin" to a "measurement time-bin" alternatively. In the locking time-bin, the resonant frequencies of the filtering cavities are locked in a conventional manner (FM-sideband locking technique [18]). Servo amplifiers keeps the filtering cavities in resonance by piezo actuators via demodulating the modulation applied to a "locking beam" (Fig. 1). In the measurement time-bin, the locking beam is completely blocked for photon counting and servo amplifiers hold the system in the same state as right before the locking beam is blocked. To perform this periodically, the locking beam first passes through an optical chopper (the chopping frequency is 500 Hz), is guided into the filtering cavities, and then returning to the same chopper again after passing them through (Fig. 1). When the locking beam passes through at the one side of optical chopper, it is blocked at the other side, and vice versa, and thus we realize the time sharing control. We also make our servo amplifiers accept external timing signals in order to be able to be synchronized to the optical chopper's driver. A different experimental approach other than the method presented here, can be found in [13].

The generated nonclassical states of light are combined with the LO at a 50:50 beam-splitter (HBS) and detected by a balanced homodyne detector with Si photodiodes (Hamamatsu S3759, anti-reflective coated at 860 nm, 99.6 % quantum efficiency). In order to improve the homodyne efficiency, the LO beam is spatially filtered by a mode cleaning cavity which yields the same spatial mode as the OPO output. The propagation loss mainly comes from the pickup of a squeezed vacuum itself (5 % at BS), and the homodyne efficiency is 98 %.

For every trigger signal from the Si-APD, a digital oscilloscope (LeCroy WaveRunner 6050A) samples homodyne signals around the time when trigger photons are detected. Each segment of data contains homodyne signals over a period $\sim 0.5\,\mu$s. They are piled one after another until $\sim$ 10000 segments fill up the oscilloscope's memory in a single run of the experiment. Each segment of the homodyne signals are sent to a PC, and then time-integrated after being multiplied by a particular temporal mode function $\Psi_0(t)$. Each Wigner function is reconstructed using the iterative maximum-likelihood estimation algorithm [19], from about 50,000 data points of quadrature amplitude.

3. Results and analysis

The temporal mode function $\Psi_0(t)$ should be chosen such that it defines the signal mode which shares the maximal entanglement with the trigger photon mode. The trigger photon mode is well localized in the time domain at least within $T \leq 1$ ns. This depends on a single-photon timing resolution of SPCM and is much shorter than the inverse bandwidth of the squeezed vacua. The bandwidth of the squeezed vacua are typically $B \sim 10$ MHz and can be characterized by the

#78885 - $15.00 USD Received 10 January 2007; revised 1 March 2007; accepted 2 March 2007

bandwidth of the OPO cavity. For such a small BT, a single mode description is valid [20]. In a good approximation, one can consider $\Psi_0(t)$ in a form [21] $\Psi_0(t) = \sqrt{\zeta_0} e^{-\zeta_0 |t|}$, assuming a trigger signal detected at $t = 0$, where $\zeta_0 \equiv (\gamma_T + \gamma_L)/2$ determines the characteristic bandwidth $\zeta_0/2\pi \sim 4.6$ MHz. Here, the leakage rates of the output coupler is $\gamma_T \sim 57$ MHz and the cavity loss rate is $\gamma_L \sim 1.2$ MHz.

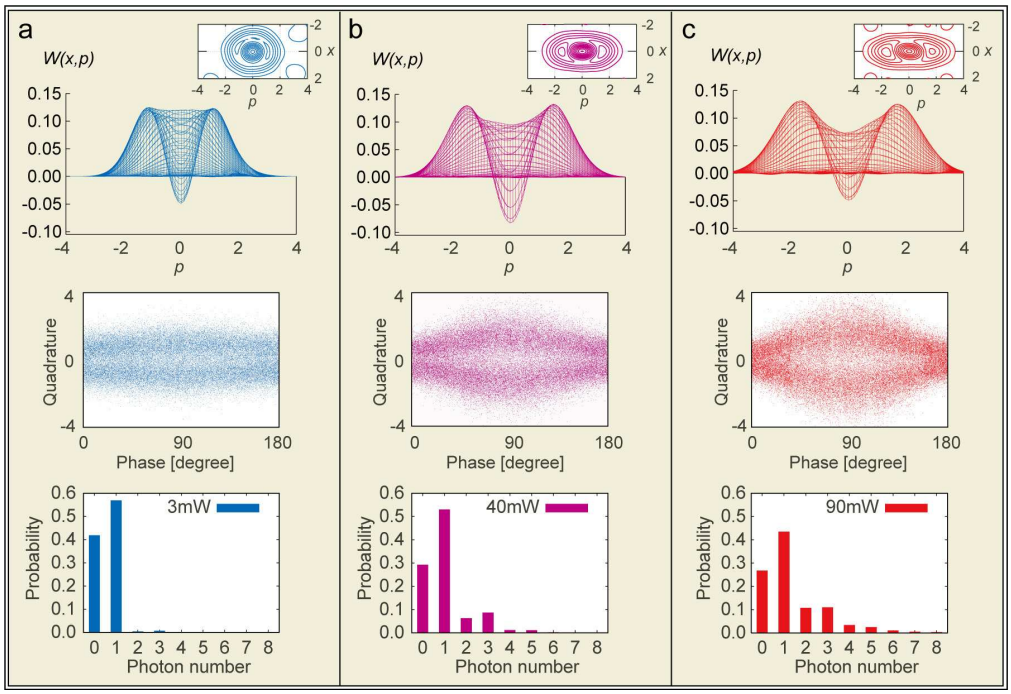

Fig. 2. Experimental Wigner functions (top panels) constructed from raw data without any correction of measurement imperfections, in the case of 5% splitting ratio. a: The single-photon state generated by -0.7dB initial squeezed vacuum. b and c: Schrödinger kittens generated by -2.6dB and -3.7dB initial squeezed vacua, respectively. The values of the Wigner function at the origin are a: $W(0,0) = -0.049$, b: $W(0,0) = -0.083$, and c: $W(0,0) = -0.048$. The insets in top panels are the contours of the Wigner functions. The middle panels are quadrature distributions obtained by homodyne detection. The bottom panels are photon-number distributions obtained by the iterative maximum-likelihood estimation.

Figure 2 shows experimental Wigner functions (top panels) and its contour plots (insets in top panels), raw data of quadrature distributions over half a period (middle panels), and photon-number distributions (bottom panels) of the photon-subtracted squeezed states. First, experimental density matrices in the Fock (photon-number state) basis are obtained from the raw data in the middle panels by using the iterative maximum-likelihood estimation. Then, the Wigner functions in the top panels can be directly calculated from the density matrices. We do not apply any corrections for measurement imperfections. The bottom panels are diagonal elements of the density matrices in the Fock basis.

The negativity of the photon-subtracted squeezed states tightly depends on a signal-to-noise (S/N) ratio of trigger photons because we cannot distinguish trigger (signal) clicks and false (noise) clicks in state preparation. False clicks just yield vacuum contributions to the generated states. A vacuum state has a Gaussian distribution of the Wigner function and a positive peak

#78885 - $15.00 USD Received 10 January 2007; revised 1 March 2007; accepted 2 March 2007

at its origin. Therefore, the negative dips of the generated states become shallow when the S/N ratio gets worse and worse, i.e., the vacuum contributions increase more and more.

Figure 2(a) corresponds to a single-photon state generated by -0.7 dB initial squeezed vacuum [29]. In such a low level of squeezing, the counting rate of trigger photons is extremely low (less than 1 kcps) and become comparable to Si-APD's dark-count rate (100 cps). Thus, the negativity in the single-photon state easily disappears even with a small amount of false clicks rather than that in the Schrödinger-kitten states. Therefore, the single-photon state particularly requires a nearly pure squeezed state generated with PPKTP, as mentioned above.

Figure 2(b) and Fig. 2(c) are for Schrödinger kittens with two kinds of amplitudes generated by -2.6 dB and -3.7 dB initial squeezed vacua [29], respectively. The odd-number enhanced distributions of photon numbers are seen as in the bottom panels. Furthermore, these two states can be seen as superpositions of mesoscopically distinct components. The large negativity is obtained in a wide range of squeezing levels.

The experimental values of the Wigner functions at their origins are Fig. 2(a): $W(0,0) = -0.049$, Fig. 2(b): $W(0,0) = -0.083$, and Fig. 2(c): $W(0,0) = -0.048$. These values are significantly improved, compared to the values with $KNbO_3$ of our group ($W(0,0) \sim 0$ at most without correction of experimental imperfections), and those of the other groups ($W(0,0) = -0.026$ without correction [12]; $W(0,0) = -0.040$ after correction [13]). Note that, in the ideal case, the photon-subtracted squeezed states include odd photon number states, and $W(0,0) = -0.32$ (for perfect setup [12]) does not vary with squeezing levels. In practice, however, optical losses are inevitable, which causes a mixing of even photon number states as seen in the bottom panels of Fig. 2(b) and Fig. 2(c). $W(0,0)$ is positive for the even photon number states. As a result, $W(0,0)$ slightly increases as the squeezing level, which can be shown by simple calculations, and was actually observed in the previous experiment [12].

4. Conclusion

In conclusion, we observed various kinds of nonclassical states from the single-photon state to Schrödinger kittens, by photon-subtraction from nearly pure squeezed vacua generated with PPKTP in an OPO. Such a state with the substantial negative dip (Fig. 2(b)), would allow one to implement quantum teleportation of nonclassicality of non-Gaussian input states [22], via the time-domain Einstein-Podolsky-Rosen correlation [23].

Another application of such states would be a breeding of Schrödinger kittens into larger cats for quantum computation by optical coherent superposition states [24], to subtract more photons by photon-number resolving detectors [25, 26, 27], or just to apply a cat-breeding protolol [28].

Acknowledgments

Authors thank K. Hayasaka, J. S. Neergaard-Nielsen, T. Aoki, H. Yonezawa, S. Suzuki, M. Takeoka and J. Mizuno for their valuable comments and suggestions. This work was supported by CREST-JST of Japan.

#78885 - $15.00 USD Received 10 January 2007; revised 1 March 2007; accepted 2 March 2007